Surface Registration via Foliation

Xiaopeng Zheng[a,c], Chengfeng Wen[b], Na Lei[a,c,d,*], Ming Ma[b], Xianfeng Gu[b,d]

[a]DUT-RU International School of Information Science and Engineering, Dalian University of Technology, Dalian 116620, China

[b]Computer Science Department, Stony Brook University, Stony Brook 11794 NY, USA

[c]Key Laboratory for Ubiquitous Network and Service Software of Liaoning Province, Dalian 116620, China

[d]Beijing Advanced Innovation Center for Imaging Technology, Capital Normal University, Beijing 100048, China

shawnxpzheng@gmail.com, chwen@cs.stonybrook.edu,

[*]Corresponding:nalei@dlut.edu.cn, Jacksoftwarecas@gmail.com, gu@cs.stonybrook.edu

Abstract

This work introduces a novel surface registration method based on foliation. A foliation decomposes the surface into a family of closed loops, such that the decomposition has local tensor product structure. By projecting each loop to a point, the surface is collapsed into a graph. Two homeomorphic surfaces with consistent foliations can be registered by first matching their foliation graphs, then matching the corresponding leaves.

This foliation based method is capable of handling surfaces with complicated topologies and large non-isometric deformations, rigorous with solid theoretic foundation, easy to implement, robust to compute. The result mapping is diffeomorphic. Our experimental results show the efficiency and efficacy of the proposed method.

1. Introduction

Surface registration plays a fundamental role in computer vision, it has a broad range of applications, such as 3D face recognition [12], shape retrieval [14], brain cortical surface registration [22], image registration [31], high resolution tracking of non-rigid motion [53] and so on.

In the past decades, researchers have intensively investigated various surface registration approaches [11, 32], such as ICP method [7, 4, 15, 43, 51, 21], dense mapping method [25, 58, 42, 33], graph matching method [18, 20, 27, 8, 9, 37], parameterizatoin based method [3, 44, 52, 57, 10, 55, 1, 49], functional based method [41, 24, 34, 45] and many other methods (e.g. [7, 12, 36]). Although surface registration techniques have been advanced greatly, it still remains challenging to handle surfaces with complicated topologies and large non-isometric deformations.

In order to tackle these challenges, this work proposes a novel method to establish diffeomorphisms between surfaces with complicated topologies, *surface registration via foliation*.

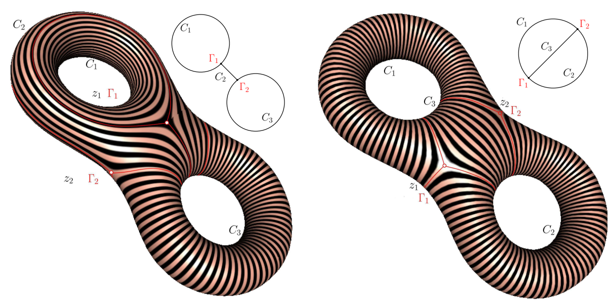

Figure 1. Foliations on a genus two surface and their corresponding projection graphs.

1.1. Proposed Approach

Foliation Fig. 1 shows the concept of foliation. Intuitively, a surface foliation decomposes the surface into a family of non-intersecting loops. Each loop is called a *leaf*. All the homotopic leaves form a cylinder, the whole surface is decomposed into cylinders $\{C_1, C_2, C_3\}$, different cylinders intersect at *critical leaves* (red leaves Γ_1, Γ_2), three cylinders meet at the *singularities* ($\{z_1, z_2\}$). We can shrink each leaf to a point to "project" the whole surface into a graph, where each cylinder is mapped to an arc, each critical leaf to a node. Furthermore, the number of leaves on each cylinder defines the length of the arc. The graph with the arc length represents the foliation.

Furthermore, the mapping from the foliation to the corresponding graph is a *generalized harmonic map*. Inversely, under some mild conditions, given a graph with the arc length, the harmonic map from the surface to the graph induces a foliation.

Registration Based on Foliation Fig. 2 shows our registration algorithmic pipeline. Given two genus g surfaces, we automatically compute $3g-3$ cutting loops on

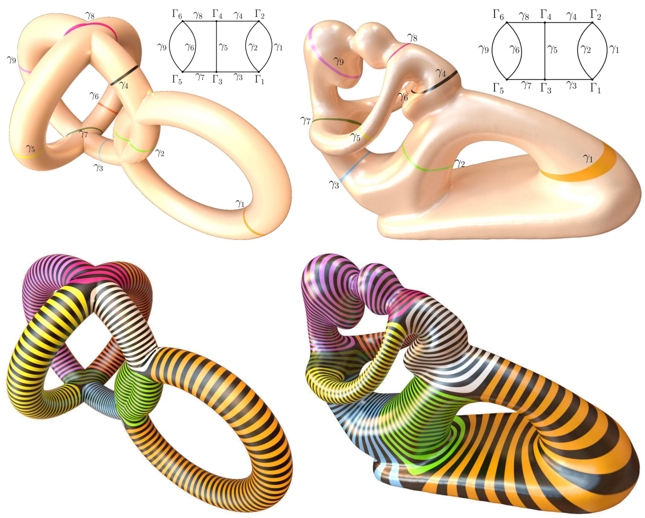

Figure 2. Surface registration based on foliation.

the surface, which divide each surface into $2g-2$ pairs of pants (genus 0 surface with 3 boundaries), this process is called the *pants decomposition*. Then we construct the corresponding *pants decomposition graph*, where each node represents a pair of pants, each arc represents a cutting loop. The consistent pants decompositions induce the same graph. We assign the arc lengths of the graph, compute the harmonic map from each surface to the graph. The harmonic mappings produce consistent foliations.

Each point on the graph corresponds to a unique leaf on the source foliation, and a leaf on the target foliation. This gives the correspondence between the leaves, furthermore, the correspondences between the singularities and the cylinders. As shown in Fig. 2, the corresponding cylinders are rendered using the same color. By further adjusting the mapping between each pair of leaves, we can achieve a global diffeomorphism between the surface.

1.2. Contributions

In summary, the main contributions are as follows:

1. It introduces a novel algorithm to compute surface registration based on foliations. This is equivalent to dimension reduction, converts surface mapping to graph matching and circle matching.
2. The method is capable of dealing with surfaces with complicated topologies, and large non-isometric deformations. It can also satisfy the landmark constraints.
3. The method has solid theoretic foundation. The registration is guaranteed to be diffeomorphic, and the existence and uniqueness of the foliation is also guaranteed.
4. The method is intrinsic, it converts the Riemannian metric of the surface to a flat metric (Euclidean geometry) with cone singularities. Comparing to methods using Riemannian geometry, it is simple and easy to implement, robust to triangulations and geometric noises in practice.

To the best of our knowledge, it is the first work to introduce foliation theory for surface registration. The computation of general foliations is based on non-linear convex optimization, hence the convergence and the global optimality has theoretic guarantees.

The main drawbacks of the current method include the non-linearity of the algorithm, and it can not directly handle partial matching for surfaces with in inconsistent boundaries.

2. Previous Works

Shape matching and registration is a well-studied field with several recent books and surveys [11, 32]. It is out of scope for this article to cover all existing shape matching and registration methods; we concentrate on the most related algorithms.

Iterative Closest Points (ICP) Method The ICP based methods find surface correspondences through an iterative procedure that starts with an initial correspondence and then repeatedly improves it by computing an aligning transformation from the correspondences and then updating the correspondences based on the transformation. These methods are most commonly used for aligning surfaces related by a rigid transformation [7], but have also been used for moderate non-rigid deformations [4, 15, 43, 51, 21]. Unfortunately, they do not guarantee that the final map is smooth or bijective (two points on one surface may map to the same point on another), and a good initial guess (which is sometimes difficult to obtain) is required to succeed in most cases.

Dense Mapping Method These methods represent a map between a pair of shapes as a point-to-point correspondence. Since it is infeasible to optimize over such correspondences directly, most methods aim to obtain a sparse set of point correspondences and extend them to dense mappings [25, 58, 42, 33]. Because sparse point correspondences are inherently discrete, common ways to enforce global consistency include preservation of various quantities between pairs or sets of points, including geodesic distances [11, 25], spectral quantities [28, 39, 40, 48, 42], or a combination of multiple geometric and topological tests [16, 6].

Graph Matching Based Methods Graph based methods [18, 20, 27, 8] are popular for surface registration. Reeb graphs based method can register high genus surfaces[9]. A Reeb graph describes the shape by storing the evolution of level sets of a given real-valued function associated to the shape. In general, the function is selected as the height function, which depends on the embedding of the surface. Our method is intrinsic, solely depends on the Riemannian metric. Furthermore, the level sets don't form a foliation, the Reeb graph method generates more singularities and more decomposed patches, and is more complicated. Our proposed foliation produces the least number of singularities and patches in theory, therefore is simpler.

Li et al. introduces the consistent pants decomposition method for registration in [37]. The surface is decomposes to pairs of pants, then the corresponding pair of pants are matched using harmonic mapping. In the process, each pair of pants are further decomposed into two topological hexagons. Therefore for a genus $g > 1$ surface, their method divides the surface into $4g - 4$ patches,ours produces $3g - 3$ cylinders. Hence foliation based method has lower complexity. We apply their automatic pants decomposition method in our pipeline.

Parameterization Based Method

Given a set of correct sparse correspondences (defined by a user or an algorithm), one can use a variety of methods to find a smooth map interpolating them. A common approach is to map both surfaces to a canonical domain where sparse feature points align to each other and then interpolate the map in that domain [3]. For example, [44] used a base coarse mesh (provided by a user) as such a domain. In their approach, the surface is cut into triangular patches defined by three geodesic curves, such that each geodesic curve is mapped to a triangle edge on a coarse base mesh. An automatic approach for creating the base domain has been developed [47, 35].

Conformal geometric methods based on the Euclidean metric have also been extensively studied [5, 57, 10, 55]. The methods in [1] and [2] uses conformal parameterization based method for surface registration with landmark constraints, the algorithms are independent of the choice of the cut graph. These methods mainly focus on genus zero surfaces. The method in Wang et al. [52] studied brain morphology with Teichmüller space coordinates where the hyperbolic conformal mapping was computed with the Yamabe flow method. Lui and Wen [38] also register high genus surfaces in their hyperbolic uniformization domains. Zeng [57] proposed a general surface registration method via the Klein model in hyperbolic space where they used the inversive distance curvature flow method to compute the hyperbolic conformal mapping. Shi et al. proposed surface registration based on a hyperbolic harmonic map in [49]. These methods are based on sophisticated curvature flow method, and the registration is carried out on hyperbolic plane. The conformal factor goes to infinity near the boundary of the hyperbolic disk, therefore, the registration algorithms are error-prone. Our proposed method uses flat metric, the computation is simpler and stabler.

Functional Based Method Functional based methods [41, 24, 34] are capable of handling surfaces with complicated topologies. Partial functional correspondence method [45] finds the partial matching between two surfaces with non-rigid, isometric deformations. It selects the corresponding subsets of the surfaces, and calculates the eigen functions of the Laplace-Beltrami operator, the corresponding points have the same values of all eigen functions. This method can handle complicated and different topology for partial matching. But this method requires the surfaces are with non-rigid but near-isometric deformation. The method can not handle surfaces with large non-isometric deformation, because the eigen functions will be very different. Our method is capable of processing shapes with large non-isometric deformations.

The current work proposes a registration method based on foliation. The existence and the uniqueness of the solution are with theoretic assurance, and the result mapping is guaranteed to be diffeomorphic. The method can handle surfaces with complicated topologies, and large non-isometric deformations. Furthermore, the algorithm is based on flat (Euclidean) metric with cone singularities, therefore simpler and more robust.

3. Theoretic Background

Our proposed method is based on fundamental concepts and theorems in conformal geometry. Here we briefly review the basic concepts. Detailed treatments can be found in [19, 50].

Riemann Surface and Conformal Mapping Given a complex function $f : \mathbb{C} \to \mathbb{C}$, $f : x + iy \mapsto u(x, y) + iv(x, y)$, if f satisfies the Cauchy-Riemann equation: $u_x = v_y$ and $u_y = -v_x$, then f is called a *holomorphic function*. If f is invertible, and f^{-1} is also holomorphic, then f is called a *bi-holomorphic function*. A surface is called a *Riemann surface*, if it is with a complex atlas $\mathcal{A}$, such that all chart transition functions are bi-holomorphic.

Holomorphic Quadratic Differential

Definition 3.1 (Holomorphic Quadratic Differentials) *Suppose S is a Riemann surface. Let Φ be a complex differential form, such that on each local chart $\{z_\alpha\}$, $\Phi = \varphi_\alpha(z_\alpha)dz_\alpha^2$, where $\varphi_\alpha(z_\alpha)$ is a holomorphic function.*

All holomorphic quadratic differentials form a linear space [19]. A point $z_i \in S$ is called a *zero* of Φ, if $\varphi(z_i)$ vanishes. A holomorphic quadratic differential has $4g - 4$ zeros, as shown in Fig. 3. For any point away from zero, we can define a local coordinates

$$\zeta(p) := \int^p \sqrt{\varphi(z)}dz. \tag{1}$$

which is the so-called *natural coordinates* induced by Φ. Suppose $\gamma \subset S$ is a curve, if $\zeta(\gamma)$ is a horizontal (vertical) line, then γ is called a *horizontal (vertical) trajectory*. If γ goes through the zeros, then it is a *critical trajectory*. If all the horizontal trajectories are finite, then Φ is called a *Strebel differential*.

Figure 3. The horizontal trajectories of a Strebel differential induces a foliation on a genus 3 surface.

Relation Between Foliation and Differential Generally speaking, given a holomorphic quadratic differential Φ, its horizontal trajectories form a foliation $\mathcal{F}$; inversely, given a foliation $\mathcal{F}$, there exists a differential Φ, whose horizontal trajectories form a foliation $\tilde{\mathcal{F}}$, such that there is an automorphism φ of the surface, φ maps $\tilde{\mathcal{F}}$ to $\mathcal{F}$.

Given a holomorphic quadratic differential Φ, the natural coordinates in Eqn. 1 induces a flat metric with cone singularities, which is denoted as $|\Phi|$. Hubbard and Masur proved the following existence of a Strebel differential with prescribed type and heights.

Theorem 3.1 (Hubbard and Masur [26]) *Suppose S is a compact Riemann surface with genus $g > 1$. Given non-intersecting simple loops $\Gamma = \{\gamma_1, \gamma_2, \cdots, \gamma_{3g-3}\}$, and positive numbers $\{h_1, h_2, \cdots, h_{3g-3}\}$, there exists a unique holomorphic quadratic differential Φ, satisfying the following :*

1. *The critical graph of Φ partition the surface into $3g-3$ cylinders, $\{C_1, C_2, \cdots, C_{3g-3}\}$, such that γ_k is the generator of C_k,*
2. *The height of each cylinder $(C_k, |\Phi|)$ equals to h_k, $k = 1, 2, \cdots, 3g-3$.*

4. Algorithm

In this section, we explain every step in the algorithm pipeline in detail.

4.1. Pants Decomposition

In our current algorithm, the pants decomposition is carried out automatically using the algorithm in [37]. Given a genus $g > 1$ closed surface S, we automatically compute the g handle loops, then find extra $2g-3$ disjoint simple loops, to form the set of cutting loops $\{\gamma_1, \gamma_2, \cdots, \gamma_{3g-3}\}$. The cutting loops segment the surface into $2g-2$ pairs of pants, $\{P_1, P_2, \cdots, P_{2g-2}\}$, to generate a *pants decomposition* of the surface. A pants decomposition can be represented as a graph G, the so-called *pants decomposition graph*, where each pair of pants is represented as a node, each simple loop is denoted by an edge. Suppose the simple loop γ_i connecting two pairs of pants P_j, P_k, then the arc of γ_i connects nodes of P_j and P_k. Then we associate a positive real number h_i for each simple loop γ_i, $1 \leq i \leq 3g-3$, namely, the corresponding edge on the pants decomposition graph. We use $(G, \mathbf{h})$ denote the pants decomposition graph G with the heights $\mathbf{h} = (h_1, h_2, \cdots, h_{3g-3})$, and call it the *weighted pants decomposition graph*. In our current implementation, we adapt the uniform heights.

4.2. Strebel Differential

Given a weighted pants decomposition graph $(G, \mathbf{h})$, consider a map $f : (S, \mathbf{g}) \to (G, \mathbf{h})$, where the length of edge γ_i is h_i. We say a point $p \in S$ a *regular point*, if its image is not any node of G, otherwise a *critical point*. The set of all critical points is denoted as Γ. Then we can define the *harmonic energy* of the mapping f,

$$E(f) := \int_{S \setminus \Gamma} |\nabla_{\mathbf{g}} f|^2 dA_{\mathbf{g}}. \tag{2}$$

The critical point of the harmonic energy is called a *harmonic map*. Wolf [56] proved the existence and the uniqueness of the harmonic map. Furthermore, the harmonic map induces a holomorphic quadratic form Φ (Hopf differential)

$$\Phi = \langle f_z, f_z \rangle dz^2.$$

By Theorem [26], the horizontal trajectories of Φ form a foliation $\mathcal{F}$. The projection graph of $\mathcal{F}$ is exactly $(G, \mathbf{h})$.

In practice, a surface is approximated by a triangular mesh $M = (V, E, F)$. We use $[v_i, v_j]$ to represent an edge connecting the vertices v_i and v_j. The weighted graph $(G, \mathbf{h})$ is with a flat metric, the length of the edge representing the loop γ_i is h_i. The harmonic energy of a map $f : M \to (G, \mathbf{h})$ is given by

$$E(f) := \frac{1}{2} \sum_{[v_i, v_j]} w_{ij} d(f(v_i), f(v_j))^2,$$

where $d(\cdot, \cdot)$ is the shortest distance between two points on the graph, w_{ij} is the *cotangent edge weight*. Suppose two faces $[v_i, v_j, v_k]$ and $[v_j, v_i, v_l]$ share the edge $[v_i, v_j]$, then

$$w_{ij} = \cot \theta_k^{ij} + \cot \theta_l^{ji},$$

where θ_k^{ij} represents the corner angle at the vertex v_k in the face $[v_i, v_j, v_k]$.

We use the *non-linear heat flow* method to compute the harmonic map. First, we deform γ_i to sweep a cylinder C_i, such that the union of all the cylinders cover the whole surface. Second, each cylinder C_i is mapped to the edge γ_i, this constructs the initial map f. Third, we diffuse the map to reduce the harmonic energy. At each step, we move the image of vertex to the *weighted geodesic center* of the images of its neighbors. Suppose after the k-th iteration, we have obtained the mapping $f_k : M \to G$ already, the vertices $\{v_j\}$'s are adjacent to the vertex v_i, the weighted geodesic center of $\{f_k(v_j)\}$'s is

$$c_k(v_i) = \text{argmin}_{q \in G} \sum_{j=1}^{n} w_{ij} d(f_k(v_j), q)^2.$$

The diffusion process moves the image of v_i to the weighted geodesic center, $f_{k+1}(v_i) \leftarrow c_k(v_i)$. The existence and the uniqueness of the harmonic map is proven in Wolf's work [56].

4.3. Registration

Given two surfaces $(\mathcal{S}, \mathbf{g})$ and $(\mathcal{T}, \mathbf{h})$, we would like to find a diffeomorphism $\varphi : \mathcal{S} \to \mathcal{T}$. We automatically compute the pants decompositions on the surfaces using the automatic algorithm in [37], with the corresponding pants decomposition graphs $G_{\mathcal{S}}$ and $G_{\mathcal{T}}$. Then the two graphs are isomorphic, $G_{\mathcal{S}} \cong G_{\mathcal{T}}$. We set the height vector $\mathbf{h}_{\mathcal{S}}$ and $\mathbf{h}_{\mathcal{T}}$ respectively, then compute the harmonic maps $f_{\mathcal{S}} : (\mathcal{S}, \mathbf{g}) \to (G_{\mathcal{S}}, \mathbf{h}_{\mathcal{S}})$ and $f_{\mathcal{T}} : (\mathcal{T}, \mathbf{h}) \to (G_{\mathcal{T}}, \mathbf{h}_{\mathcal{T}})$. The harmonic maps induce the Strebel differentials $\Phi_{\mathcal{S}}$ and $\Phi_{\mathcal{T}}$. The critical trajectories of $\Phi_{\mathcal{S}}$ are $\Gamma_{\mathcal{S}}$, those of $\Phi_{\mathcal{T}}$ are $\Gamma_{\mathcal{T}}$. The critical trajectories partition the surfaces into $2g-2$ cylinders,

$$\mathcal{S} \setminus \Gamma_{\mathcal{S}} = \bigcup_{k=1}^{2g-2} \mathcal{C}_{\mathcal{S}}^k, \quad \mathcal{T} \setminus \Gamma_{\mathcal{T}} = \bigcup_{k=1}^{2g-2} \mathcal{C}_{\mathcal{T}}^k$$

The Strebel differentials $\Phi_{\mathcal{S}}$ and $\Phi_{\mathcal{T}}$ induce flat metrics, $|\Phi_{\mathcal{S}}|$ and $|\Phi_{\mathcal{T}}|$ respectively.

The restriction of $\Phi_{\mathcal{S}}$ on each cylinder $\mathcal{C}_{\mathcal{S}}^k$ is a harmonic function, then we can define a harmonic 1-form

$$\omega_k := d\Phi_{\mathcal{S}}|_{\mathcal{C}_{\mathcal{S}}^k},$$

then we use the Hodge star operator to act on ω_k to get the conjugate harmonic 1-form ${}^*\omega_k$, then pair them to form a holomorphic 1-form $\Omega_k := \omega_k + \sqrt{-1}{}^*\omega_k$. Then the union of all Ω_k^2's give the Strebel differential $\Phi_{\mathcal{S}}$, $\Omega_k \bar{\Omega}_k$ gives the flat metric $|\Phi_{\mathcal{S}}|$. We use the method in [30] to compute the Hodge star operator and discrete holomorphic 1-form Ω_k.

For each pair of flat cylinders, we can construct a harmonic map using conventional harmonic mapping method [54]

$$\varphi_k : (\mathcal{C}_{\mathcal{S}}^k, |\Phi_{\mathcal{S}}|) \to (\mathcal{C}_{\mathcal{T}}^k, |\Phi_{\mathcal{T}}|),$$

with consistent boundary conditions, such that the zero points of $\Phi_{\mathcal{S}}$ on the boundaries of $\mathcal{C}_{\mathcal{S}}^k$ are mapped to the zero points of $\Phi_{\mathcal{T}}$ on the boundaries of $\mathcal{C}_{\mathcal{T}}^k$.

All the harmonic maps φ_k's are glued together to form a global piecewise harmonic map $\varphi : (\mathcal{S}, |\phi_{\mathcal{S}}|) \to (\mathcal{T}, |\phi_{\mathcal{T}}|)$. By construction, the mapping φ is a homeomorphism. Furthermore, the global map can be further diffused under the metric ($|\phi_{\mathcal{T}}|$ on the target surface) to become a global harmonic map. According to the harmonic map theorem [46], the harmonic map exists and is unique, furthermore diffeomorphic. Details can be found in Algorithm 1.

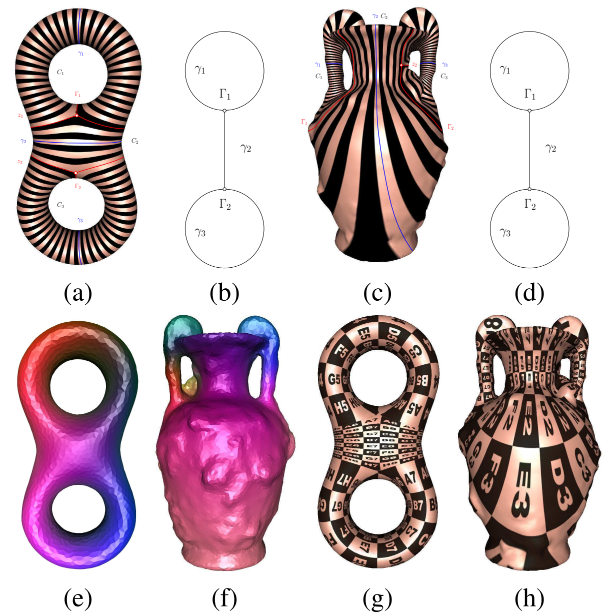

Figure 4. Registration between the eight surface and the amphora surface.

Fig. 2 and Fig. 4 illustrate the process of surface registration. Fig. 4 shows a pair of genus two surfaces, the eight surface (a) and the amphora surface (c). The pants decompositions are automatically computed, the cutting loops are $\{\gamma_1, \gamma_2, \gamma_3\}$ (blue curves in frames (a) and (c)) on both surfaces, the pants decomposition graph is shown in (b) and (d). The user specifies the height function, and compute the harmonic maps from the surfaces to the graphs, which induces foliations as shown in (a) and (c), the zero points are $\{z_1, z_2\}$, the critical trajectories are $\{\Gamma_1, \Gamma_2\}$, the cylinders are $\{C_1, C_2, C_3\}$. The corresponding cylinders are registered using harmonic maps with consistent boundary conditions, under the flat metrics induced by the Strebel differentials. The piecewise harmonic maps are glued together, and smoothed out. The resultant global diffeomorphism is illustrated by consistent color map in frames (e) and (f), the source point and the image point share the same color. Frame (g) and (h) show the mapping using consistent texture mapping within each cylinder. Each checker has an alphabetic and numerical label, which shows the correspondence and the distortions of the mapping. By visual inspection, we can see the smoothness of the registration.

5. Experimental Results

In this section, we report our experimental results. We have tested our algorithm on surfaces scanned from real life [17] and reconstructed from medical images. Our algorithm is implemented using generic C++, the numerical computa-

Algorithm 1 Surface Registration Algorithm Pipeline.

Require: : Closed surfaces $\mathcal{S}$ and $\mathcal{T}$ with genus $g > 1$
Ensure: : A diffeomorphism $\varphi : \mathcal{S} \to \mathcal{T}$

1. Construct the pants decomposition of $\mathcal{S}$, with the graph $G_\mathcal{S}$, assign the height function $\mathbf{h}_\mathcal{S}$,
2. Construct the pants decomposition of $\mathcal{T}$, with the graph $G_\mathcal{T}$, assign the height function $\mathbf{h}_\mathcal{T}$,
3. Compute the harmonic map $u_\mathcal{S} : \mathcal{S} \to G_\mathcal{S}$, which induces a Strebel differential $\Phi_\mathcal{S}$ with critical trajectory $\Gamma_\mathcal{S}$,
6. Compute the harmonic map $u_\mathcal{T} : \mathcal{T} \to G_\mathcal{T}$, which induces a Strebel differential $\Phi_\mathcal{T}$ with critical trajectory $\Gamma_\mathcal{T}$,
7. Slice $\mathcal{S}$ along the critical trajectories $\Gamma_\mathcal{S}$ to obtain cylindrical decomposition, $\mathcal{S} \setminus \Gamma_\mathcal{S} = \cup_{k=1}^{2g-2} C_\mathcal{S}^k$,
8. Slice $\mathcal{T}$ along the critical trajectories $\Gamma_\mathcal{T}$ to obtain cylindrical decomposition, $\mathcal{T} \setminus \Gamma_\mathcal{T} = \cup_{k=1}^{2g-2} C_\mathcal{T}^k$,

for all $k = 1, 2, \ldots, 2g - 2$ **do**
  9. Construct a harmonic maps $\varphi_k : (C_\mathcal{S}^k, |\Phi_\mathcal{S}|) \to (C_\mathcal{T}^k, |\Phi_\mathcal{T}|)$
end for

10: Glue all the local harmonic maps together to form the global map $\varphi : (\mathcal{S}, |\Phi_\mathcal{S}|) \to (\mathcal{T}, |\Phi_\mathcal{T}|)$.
11: Diffuse φ to a harmonic map using non-linear heat diffusion method.

tion is based on Eigen library [23]. All our experiments are performed on a desktop computer with Intel(R) Core(TM) i7-4770 3.4GHz CPU and 16GB RAM.

5.1. Robustness Testing

In order to test the robustness of our foliation based method, we conducted an experiment as shown in Fig. 5. The input genus 2 mesh is with good quality triangulation, the foliation is calculated as shown in the top row. We modify the connectivity to reduce the triangulation quality to introduce skinny faces, but foliation is slightly affected as shown in the middle row. Then we add geometric noises to the shape by randomly moving every point along its normal, the perturbation distance is about 3% of the diagonal of the bounding box. The foliation of the bumpy surface looks very similar to original one. Because the computation of foliations is equivalent to solve an elliptic partial differential equation, the solution is stable and robust to the triangulation quality and geometric noise.

5.2. High Genus Testing

Fig. 6 and Fig. 7 show the registration result between the eight model and the girl sculpture. Fig. 6 frame (a) and (c) show the foliations, (b) and (d) illustrate the registration by consistent color encoding, which shows the smoothness of the mapping. Fig. 7 shows the correspondence by consistent texture mapping. Each checker on the texture has both alphabetic and numerical labels. By examining the labels of the checkers, one can verify the correspondence and visualize the distortions.

Similarly, Fig. 8 shows the registration result between the genus two surfaces, the amphora model and the star cup. Fig. 2 shows the mapping between genus 4 surfaces. These

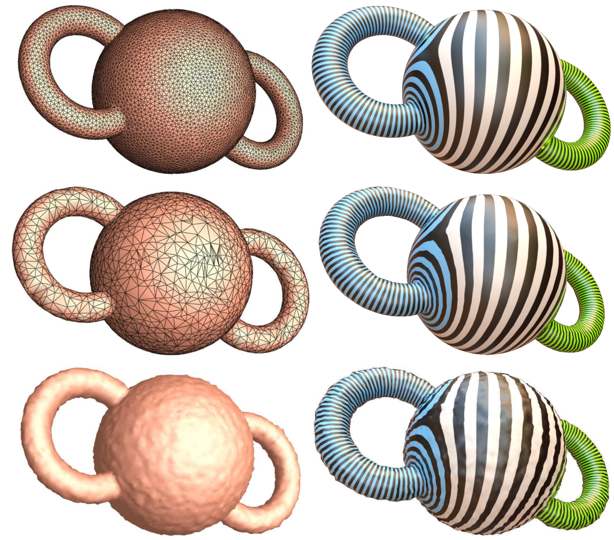

Figure 5. Robustness testing.

experiments demonstrate that our method can handle high genus surfaces.

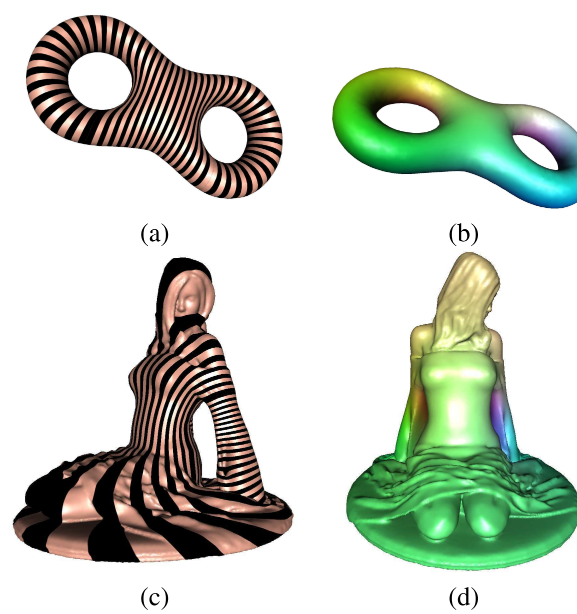

Figure 6. The foliation of the eight surface (a), the foliation of girl sculpture surface (b). The mapping is illustrated by consistent color encoding (c) and (d).

5.3. Landmarks Constraints Testing

Fig. 9 shows registration of surfaces with feature points and bundaries. The 11 cat models from TOSCA datasets [13] are with different poses, and with non-rigid but near-isometric deformations. There are 7 features points like the tips of the ears and the tail, 2 boundary landmark curves, which are treated as constraints for the registration. Each cat surface is decomposed into 15 cylinders, the corresponding cylinders are color-encoded similarly. By visual verification, we can see the correspondences among the leaves, and

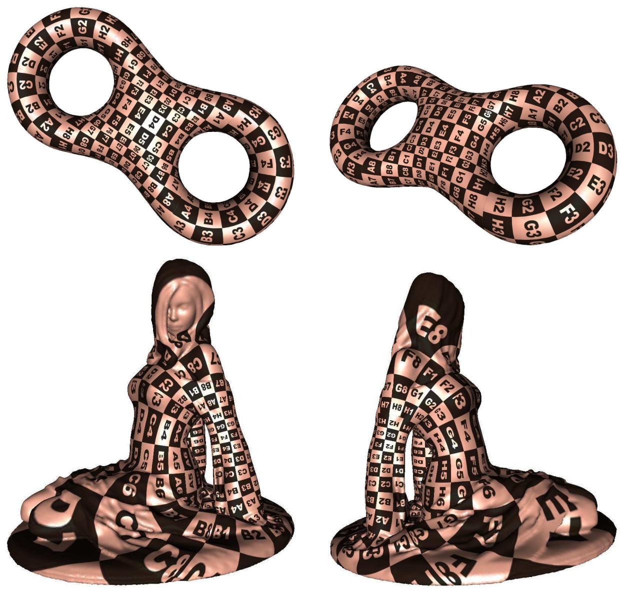

Figure 7. The diffeomorphism between the eight surface and the girl sculpture.

the features and landmarks. Some cats models have self-intersections, which doesn't affect our algorithm, since our method solely depends on the Riemannian metric, not the embedding.

Fig. 10 and 11 show another example for registering genus zero surfaces with landmark curves. The human cortical surface is with three consistent landmark Succi curves (red curves) in the top row in Fig. 10. Then we perform double covering technique [29] to covert each of them to a genus two closed surface and compute the foliation on the double cover, as shown in the bottom row in Fig. 10. The registration results between two cortical surfaces is illustrated by consistent color-encoding in Fig. 11.

We have perform the registration between each pair of cortical surfaces in a database containing 40 brains, and all 780 registrations are carried out automatically and successfully. This further demonstrates the robustness of our algorithm.

5.4. Efficiency Testing

We report the running time of our algorithm in this section. The time of computing the foliation are shown in Table 1. The timing for the registration in the algorithm pipeline are as follows: the mapping between the eight surface to ampora model is $2.32s$; eight surface to the girl sculpture $30.188s$; the star cup model to the amphora model $64.244s$; the cortical surfaces $205.05s$.

5.5. Comparison

We compare our method with the hyperbolic harmonic map algorithm introduced in [49] in terms of robustness, efficiency and accuracy.

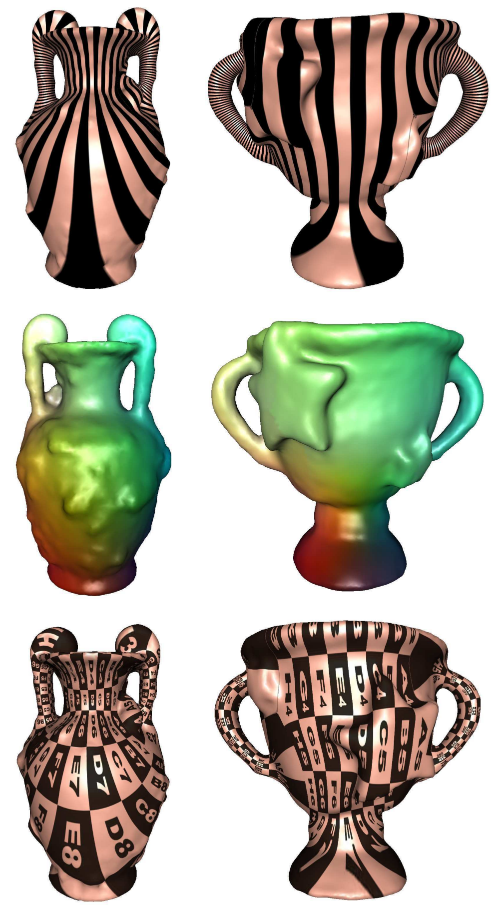

Figure 8. Registration between the star cup surface and the amphora surface. The first row shows the foliation on both model. The second row is the registration result shown in color coding. The third row shows the mapping result using consistent texture mapping.

Model	# of vertices	# of faces	Time(second)
eight	3776	7556	5.6
amphora	10565	21134	15
starcup	31272	62548	33
brain	30988	61972	70
cat	27894	55712	359
sculpture girl	80000	160004	259

Table 1. The computation time of foliations of different models.

The hyperbolic harmonic map algorithm depends on hyperbolic Ricci flow, which is sensitive to the meshing quality. It may fail on surfaces with low mesh qualities. In contrast, our method is based on harmonic mapping, which is more robust to the meshing quality and succeeds in all cases.

The Ricci flow method is highly non-linear, which is time-consuming with the total time $310s$; our method is more efficient with the total time $275s$ on the same model.

Figure 9. Registration with feature points and boundaries.

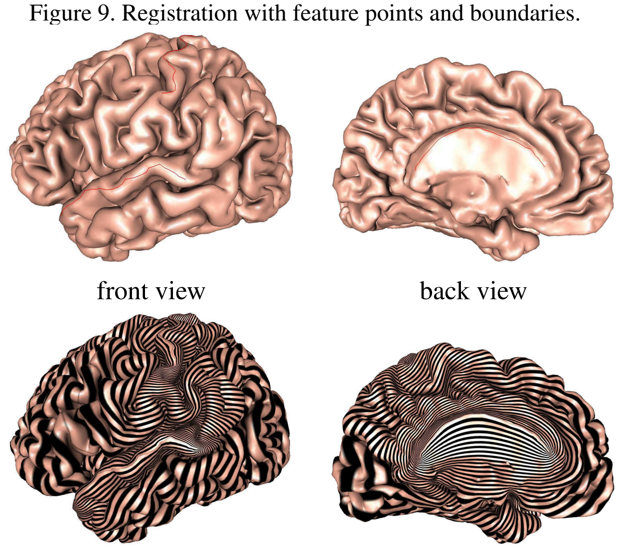

Figure 10. The landmark curves (top row) and the foliation (bottom row) on a human brain surface.

Furthermore, we measure the registration quality by the *curvature distortion metric*. Basically, a mapping between two surfaces will pull back the Gaussian curvature and mean curvature on the target to the source. Then on the source surface, we compute the L^2 distance between the source curvature and the pulled-back curvature, which is the curvature distortion distance. If the registration is an isometric mapping, then the L^2 distance of Gaussian curvatures is 0; if the registration is a rigid motion in $\mathbb{R}^3$, then both Gaussian and mean curvature distances are 0. We compute the distribution of the curvature difference, and show the histograms in Fig. 12. It is obvious that the curvature differences distribution of our method highly concentrates near the 0, the distribution of the hyperbolic harmonic mapping method in [49] is much more spread out. This demonstrates that our method achieves higher accuracy.

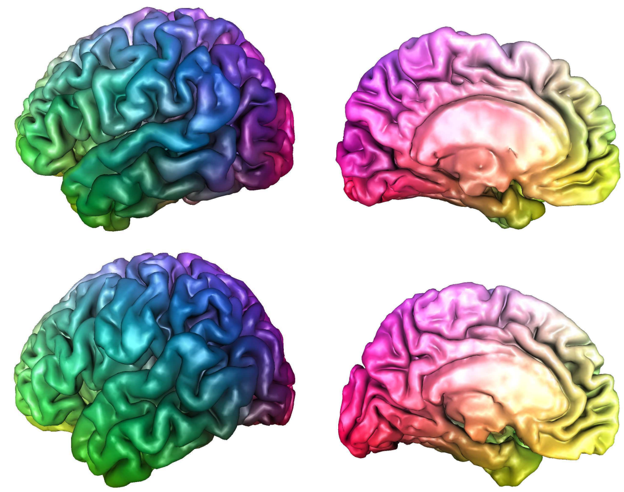

Figure 11. The color-encoded registration results of the human cortical surfaces. The first row shows the source brain while the second row shows the target.

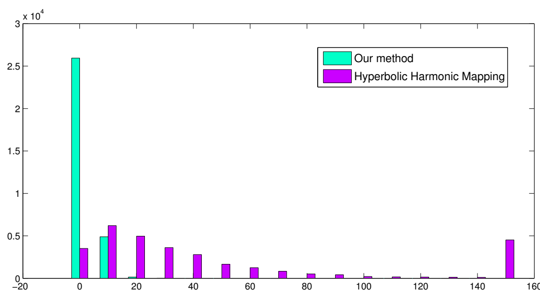

Figure 12. The distribution of the curvature difference. The last purple bar shows the number of vertices whose curvature difference are equal or greater than 150 in the hyperbolic harmonic mapping method.

6. Conclusion

This work introduces a novel surface registration algorithm based on foliation theory. The surface is decomposed into a family of leaves (loops), the arrangement of which is represented as a graph. Surface registration is carried out by matching the graphs first, then match the leaves. This method can handle surfaces with complicated topologies and large non-isometric deformations; it has rigorous theoretic foundation to guarantee the existence and the uniqueness of the solution, the resulting mapping is diffeomorphic; the algorithm is simple to implement, robust to compute. Experimental results demonstrates the efficinecy and efficacy of the proposed method.

On a surface, there are infinite many foliations. In theory, given a pair of homeomorphic surfaces, one can choose unique foliations on each of them, such that the mapping has the least distortions. In the future, we will explore how to find the optimal foliations to improve the mapping qualities.

References

[1] N. Aigerman and Y. Lipman. Orbifold tutte embeddings. *ACM Trans. Graph.*, 34(6):190:1–190:12, Oct. 2015.

[2] N. Aigerman, R. Poranne, and Y. Lipman. Seamless surface mappings. *ACM Trans. Graph.*, 34(4):72:1–72:13, July 2015.

[3] M. Alexa. Recent advances in mesh morphing. *Comput. Graph. Forum*, 21(2):173–196, 2002.

[4] B. Allen, B. Curless, and Z. Popović. The space of human body shapes: reconstruction and parameterization from range scans. *ACM Trans. Graph.*, 22(3):587–594, Jul 2003.

[5] S. Angenent, S. Haker, A. Tannenbaum, and R. Kikinis. Conformal geometry and brain flattening. In *MICCAI*, pages 271–278, Sep. 1999.

[6] O. K.-C. Au, C.-L. Tai, D. Cohen-Or, Y. Zheng, and H. Fu. Electors voting for fast automatic shape correspondence. *Comput. Graph. Forum*, 29(2):645–654, 2010.

[7] P. J. Besl and N. D. Mckay. A method for registration of 3D shapes. *TPAMI*, 14(2), Feb. 1992.

[8] D. Bespalov, A. Shokoufandeh, W. C. Regli, and W. Sun. Scalespace representation of 3D models and topological matching. In *Proceedings of the 8th ACM Symposium on Solid Modeling and Applications. ACM Press, Seattle, Washington*, pages 208–215, 2003.

[9] S. Biasotti, S. Marini, M. Spagnuolo, and B. Falcidieno. Subpart correspondence by structural descriptors of 3d shapes. *Computer-Aided Design*, 38(9):1002–1019, 2006.

[10] D. M. Boyer, Y. Lipman, E. St Clair, J. Puente, B. A. Patel, T. Funkhouser, J. Jernvall, and I. Daubechies. Algorithms to automatically quantify the geometric similarity of anatomical surfaces. *Proc. Natl. Acad. Sci. U.S.A.*, 108:18221–18226, Nov 2011.

[11] A. Bronstein, M. Bronstein, and R. Kimmel. *Numerical Geometry of Non-Rigid Shapes*. 2008.

[12] A. M. Bronstein, M. M. Bronstein, and R. Kimmel. Generalized multidimensional scaling: a framework for isometry-invariant partial surface matching. *Proc. Natl. Acad. Sci. U.S.A.*, 103(5):1168–1172, Jan 2006.

[13] A. M. Bronstein, M. M. Bronstein, and R. Kimmel. *Numerical geometry of non-rigid shapes*. Springer Science & Business Media, 2008.

[14] M. M. Bronstein and A. M. Bronstein. Shape recognition with spectral distances. *IEEE TPAMI*, 33(5):1065–1071, May 2011.

[15] B. J. Brown and S. Rusinkiewicz. Global non-rigid alignment of 3-d scans. In *ACM SIGGRAPH 2007 papers*, SIGGRAPH '07, 2007.

[16] A. Dubrovina and R. Kimmel. Approximately isometric shape correspondence by matching pointwise spectral features and global geodesic structures. *Advances in Adaptive Data Analysis*, 3(1-2):203–228, 2011.

[17] B. Falcidieno. Aim@ shape project presentation. In *Shape Modeling Applications, 2004. Proceedings*, page 329. IEEE, 2004.

[18] T. Fan, G. Medioni, and R. Nevatia. Recognizing 3d objects using surface description. *IEEE Transactions on Pattern Analysis and Machine Intelligence*, 11(11):1140–1157, 1989.

[19] H. M. Farkas and I. Kra. *Riemann Surfaces*. Springer, 2004.

[20] T. Funkhouser, M. Kazhdan, P. Shilane, P. Min, W. Kiefer, A. Tal, S. Rusinkiewicz, and D. Dobkin. Modeling by example. *ACM Transactions on Graphics*, 23(3):652–663, 2004.

[21] A. Golovinskiy and T. Funkhouser. Consistent segmentation of 3d models. In *Computers & Graphics, IEEE SMI 2009 proceedings, (33)3*, pages 262–269, 2009.

[22] X. Gu, Y. Wang, T. F. Chan, P. M. Thompson, and S.-T. Yau. Genus zero surface conformal mapping and its application to brain surface mapping. *IEEE Trans. Med. Imag.*, 23(8):949–958, Aug. 2004.

[23] G. Guennebaud, B. Jacob, et al. Eigen v3. http://eigen.tuxfamily.org, 2010.

[24] Q. Huang, F. Wang, and L. Guibas. Functional map networks for analyzing and exploring large shape collections. *Acm Transactions on Graphics*, 33(4):36, 2014.

[25] Q.-X. Huang, B. Adams, M. Wicke, and L. J. Guibas. Nonrigid registration under isometric deformations. In *Proceedings of the Symposium on Geometry Processing*, SGP 08, pages 1449–1457, 2008.

[26] J. Hubbard and H. Masur. Quadratic differentials and foliations. *Acta Math.*, (142):221–274, 1979.

[27] D. Huber, A. Kapuria, R. Donamukkala, and M. Hebert. Parts-based 3D object classification. In *Proceedings of the International Conference on Computer Vision*, pages 82–89, 2004.

[28] V. Jain, H. Zhang, and O. van Kaick. Non-rigid spectral correspondence of triangle meshes, 2006.

[29] M. Jin, J. Kim, F. Luo, and X. Gu. Discrete surface Ricci flow. *IEEE Trans. Visual Comput. Graphics*, 14(5):1030–1043, Sept.-Oct. 2008.

[30] M. Jin, Y. Wang, S.-T. Yau, and X. Gu. Optimal global conformal surface parameterization. In *Proceedings of the IEEE Visualization 2004*, pages 267–274. IEEE Computer Society, 2004.

[31] A. Joshi, D. Shattuck, P. Thompson, and R. Leahy. Surface-constrained volumetric brain registration using harmonic mappings. *IEEE Trans. Med. Imag.*, 26(12):1657–1669, Dec. 2007.

[32] O. V. Kaick, H. Zhang, G. Hamarneh, and D. Cohen-or. A survey on shape correspondence, 2011.

[33] V. G. Kim, Y. Lipman, and T. Funkhouser. Blended intrinsic maps. In *ACM SIGGRAPH 2011*, SIGGRAPH '11, pages 79:1–79:12, 2011.

[34] A. Kovnatsky, M. M. Bronstein, X. Bresson, and P. Vandergheynst. Functional correspondence by matrix completion. *Computer Science*, pages 905–914, 2015.

[35] V. Kraevoy and A. Sheffer. Cross-parameterization and compatible remeshing of 3d models. *ACM Trans. Graph.*, 23(3):861–869, Aug 2004.

[36] S. Kurtek, E. Klassen, J. C. Gore, Z. Ding, and A. Srivastava. Elastic Geodesic Paths in Shape Space of Parametrized Surfaces. *IEEE Trans Pattern Anal Mach Intell*, Nov 2011.

[37] X. Li, X. Gu, and H. Qin. Surface mapping using consistent pants decomposition. *IEEE Trans. Vis. Comput. Graph.*, 15(4):558–571, 2009.

[38] L. M. Lui and C. Wen. Geometric registration of high-genus surfaces. *SIAM Journal on Imaging Sciences*, 7(1):337–365, 2014.

[39] D. Mateus, R. Horaud, D. Knossow, F. Cuzzolin, and E. Boyer. Articulated shape matching using laplacian eigenfunctions and unsupervised point registration. In *Computer Vision and Pattern Recognition, 2008. CVPR 2008. IEEE Conference on*, pages 1–8, 2008.

[40] F. Mémoli. Spectral Gromov-Wasserstein distances for shape matching. In *Computer Vision Workshops (ICCV Workshops), 2009 IEEE 12th International Conference on*, pages 256–263. IEEE, 2009.

[41] M. Ovsjanikov, M. Ben-Chen, J. Solomon, A. Butscher, and L. Guibas. Functional maps:a flexible representation of maps between shapes. *Acm Transactions on Graphics*, 31(4):1–11, 2012.

[42] M. Ovsjanikov, Q. Mrigot, F. Mmoli, and L. J. Guibas. One point isometric matching with the heat kernel. *Comput. Graph. Forum*, 29(5):1555–1564, 2010.

[43] M. Pauly, N. J. Mitra, J. Giesen, M. Gross, and L. J. Guibas. Example-based 3d scan completion. In *Proceedings of the third Eurographics symposium on Geometry processing*, SGP '05, 2005.

[44] E. Praun, W. Sweldens, and P. Schröder. Consistent mesh parameterizations. In *Proceedings of the 28th annual conference on Computer graphics and interactive techniques*, pages 179–184, 2001.

[45] E. Rodola, L. Cosmo, M. M. Bronstein, A. Torsello, and D. Cremers. Partial functional correspondence. *Computer Graphics Forum*, 36(1):222–236, 2017.

[46] R. Schoen and S.-T. Yau. *Lectures on Harmonic Maps*. International Press, 1997.

[47] J. Schreiner, A. Asirvatham, E. Praun, and H. Hoppe. Intersurface mapping. ACM SIGGRAPH, pages 870–877, 2004.

[48] A. Sharma and R. Horaud. Shape matching based on diffusion embedding and on mutual isometric consistency. In *Computer Vision and Pattern Recognition Workshops (CVPRW), 2010 IEEE Computer Society Conference on*, pages 29–36, 2010.

[49] R. Shi, W. Zeng, Z. Su, H. Damasio, Z. Lu, Y. Wang, S.-T. Yau, and X. Gu. Hyperbolic harmonic mapping for constrained brain surface registration. In *Computer Vision and Pattern Recognition (CVPR), 2013 IEEE Conference on*, pages 2531–2538. IEEE, 2013.

[50] K. Strebel. *Quadratic Differentials*. Springer-Verlag, 1984.

[51] A. Tevs, M. Bokeloh, M. Wand, A. Schilling, and H. P. Seidel. Isometric registration of ambiguous and partial data. In *CVPR 2009.*, pages 1185–1192, 2009.

[52] Y. Wang, W. Dai, X. Gu, T. F. Chan, A. W. Toga, and P. M. Thompson. Studying brain morphology using Teichmüller space theory. In *ICCV*, pages 2365–2372, 2009.

[53] Y. Wang, M. Gupta, S. Zhang, S. Wang, X. Gu, D. Samaras, and P. Huang. High resolution tracking of non-rigid motion of densely sampled 3d data using harmonic maps. *Int. J. Comput. Vision*, 76(3):283–300, 2008.

[54] Y. Wang, M. Gupta, S. Zhang, S. Wang, X. Gu, D. Samaras, and P. Huang. High resolution tracking of non-rigid motion of densely sampled 3d data using harmonic maps. *IJCV*, 76, 2008.

[55] Y. Wang, J. Shi, X. Yin, X. Gu, T. F. Chan, S. T. Yau, A. W. Toga, and P. M. Thompson. Brain surface conformal parameterization with the Ricci flow. *IEEE TMI*, 31(2):251–264, 2012.

[56] M. Wolf. On realizing measured foliations via quadratic differentials of harmonic maps to r-trees. *J. D'Analyse Math*, pages 107–120, 1996.

[57] W. Zeng, D. Samaras, and X. Gu. Ricci flow for 3D shape analysis. *IEEE TPAMI*, 32:662–677, 2010.

[58] Y. Zeng, C. Wang, Y. Wang, X. Gu, D. Samaras, and N. Paragios. Dense non-rigid surface registration using high-order graph matching. In *Computer Vision and Pattern Recognition (CVPR), 2010 IEEE Conference on*, pages 382–389, 2010.